

Polyelectrolyte Effects in Model Photoresist Developer Solutions: Roles of Base Concentration and Added Salts

Vivek M. Prabhu ^{a*}, Ronald L. Jones ^a, Eric K. Lin ^a, Christopher L. Soles ^a, Wen-li Wu ^a,
Dario L. Goldfarb ^b and Marie Angelopoulos ^b

^a Polymers Division, National Institute of Standards and Technology, Gaithersburg, MD 20899

^b IBM T.J. Watson Research Center, Yorktown Heights, NY 10598

ABSTRACT

We demonstrate that poly(4-hydroxystyrene) and (5, 15, and 20) % *tert*-butoxycarboxy protected copolymers are polyelectrolytes when dissolved in aqueous base solutions. The polyelectrolyte effect is quantified through the observation of a correlation peak, measured with small-angle neutron scattering. Polyelectrolyte effects are weakened with added salts and excess base. These studies emphasize that salt additives screen the electrostatic interactions, while pH leads to the ionization of the chain. Solvent quality is quantified and the chain configurations are measured in the limit of high ionic strength. It is speculated that the developer-resist interactions will play an important role in development-induced roughness, hence these equilibrium solution measurements can serve a predictive function for future photoresists dissolution models incorporating solvent quality as a parameter.

Keywords: polyelectrolyte, photoresist, developer, roughness, additives, solvent quality, neutron scattering

1. INTRODUCTION

This paper highlights polyelectrolyte effects induced by developer-resist interactions. It is well known the high pH of the aqueous base developer solution renders poly(hydroxystyrene) (PHOSt) soluble. From organic chemistry tables, the pKa of a phenol ¹ proton is 10. Thus, for solutions with pH greater than 10, the equilibrium conditions favor the deprotonated state. Since, the pH of a 0.26 M tetramethyl ammonium hydroxide (TMAH) solution is 13.3, equilibrium conditions strongly favor the conjugate base form. *This chemical equilibrium state is the origin of the intended miscibility.* Bare PHOSt is not miscible in pure water. When charged monomers are covalently connected into a polymer, the influence of long-range correlations between monomers is important. Simple acid-base equilibrium, based upon well-defined chemical equations, neglect these correlations. This behavior is studied within the context of charged polymers, polyelectrolytes.

The long-ranged monomer-monomer correlations are measured with small-angle neutron scattering (SANS). We utilize this technique to understand the roles of dissolution additives in aqueous base developers. This paper highlights differences between the ionized form of model photoresist solutions and its unionized counterpart in organic solvents. These results may have direct implications for advancements in photoresists dissolution theory and understanding.

One fundamental step needed in current dissolution models is the role of solvent quality at the resist-developer interface. The next generation of photoresists exhibits significant swelling and new dissolution features, not observed for the 248 nm PHOSt-PBOCSt system ². Methodologies to reduce this swelling involve dissolution inhibitors and/or modifying agents. However, solvent and base penetration into the resist, neglected in current models, will need to be incorporated into models to fully understand and control the multi-step dissolution process observed for next generation resists². The physics of this penetration front require additional kinetic and equilibrium studies.

* Corresponding author. vprabhu@nist.gov, Tel.: (301) 975-3657; fax (301) 975-3928.

A recent advancement in the dissolution model framework is the incorporation of electrostatic effects at the resist-developer interface. By modeling a uniformly charged resist interface, the consequence is the formation of an electrostatic double layer. For the case of a weakly acidic photoresist, the double layer modeling leads to a depletion of aqueous base ions at the similarly charged surface. This reduces the local pH at the surface, leading to a lower surface charge density for a given base concentration. This electrical feedback loop of ionization-dissolution has improved the quantitative agreement between experiment and simulation³.

A kinetic model for positive-tone resist dissolution and roughening utilizes the critical ionization criteria to understand the relation of aerial image contrast (compositional deprotection gradients) on roughness and dissolution with a series of reaction-rate kinetic steps⁴. This theory is extendable to include association kinetics (gelation), which may be critical for agreement with next generation resists.

This paper identifies and initiates discussion of dissolution with respect to charged polymer physics, polyelectrolytes, and its importance in understanding photoresist-developer solutions. We highlight the polyelectrolyte effects in this paper and discuss the consequences within the current dissolution models. We emphasize the polymeric phase behavior in terms of solvent quality and its relation to roughness.

2. EXPERIMENTAL

The details of the polymers used in these studies, such as the weight-average relative molecular weight are provided in Table I. The deuterated poly(4-hydroxystyrene) (d_3 -PHOST), deuterated along the main chain, was custom synthesized by Polymer Source, Inc., Dorval, Quebec⁵. The polymers with varying degree of *tert*-butoxycarboxy (t-BOC) protection are fully protonated, and characterized by GPC. To prepare samples for the equilibrium solution measurements, the dry powder was dissolved directly in aqueous base solutions with and without added salts and diluted to known concentrations. Tetramethyl ammonium hydroxide (TMAH) solutions were prepared by dilution of a stock solution (mass fraction of 10%), purchased from Aldrich Chemicals, using deionized water with resistivity 18.0 M Ω -cm purified by a Milli-Q UF Plus system⁵. Sodium hydroxide (NaOH) and potassium hydroxide (KOH) solutions were prepared by quantitative addition of analytical grade salt pellets to a known volume of deionized water to achieve the desired normality of 0.26 N. To prepare solutions with added salts, potassium chloride (KCl) and sodium chloride (NaCl) were dissolved directly in the corresponding aqueous base solutions: NaCl in NaOH and TMAH solutions and KCl in KOH solutions. Similar methods were used to prepare solutions in propylene glycol methyl ether acetate (PGMEA) and deuterated acetone.

Small-angle neutron scattering (SANS) was performed on the NG1 guide 8 m and NG3 30 m instruments at the NIST Center for Neutron Research (NCNR). On both instruments the wavelength of neutron used was 6.0 Å with a spread ($\Delta\lambda/\lambda$) of 0.12 on NG1 and 0.15 on NG 3. The scattered intensity is measured as a function of wave vector defined by $q = (4\pi/\lambda) \sin(\theta/2)$, where θ is the scattering angle. The details with regards to data collection and reduction can be found elsewhere⁶. The uncertainties in scattered intensity are calculated as the estimated standard deviation of the mean. In the case where the limits are smaller than the plotted symbols, the limits are left out for clarity. Fits of the scattering data are made by a weighted least-squares minimization and the error corresponds to one standard deviation to the fit.

3. BACKGROUND

3.1. Dilute Neutral Polymer Solutions

We measured the scattering by model photoresist polymers in a typical casting solvent propylene glycol methyl ether acetate (PGMEA), deuterated acetone and several aqueous base developer solutions: sodium hydroxide (NaOH), potassium hydroxide (KOH), and tetramethyl ammonium hydroxide (TMAH), with and without added salts. The coherent neutron scattering is feasible due to the scattering length density difference between PHOST (b_m/v_m) and the solvent (b_s/v_s). SANS experiments measure the monomer-monomer correlations denoted by the total scattering structure factor $S_T(q)$. Here we present the scattering equation in which C_m is the monomer concentration and N the degree of polymerization,

$$I(q) = \left(\frac{b_m}{v_m} - \frac{b_s}{v_s} \right)^2 C_m N S_T(q) \quad (1)$$

In the limit of dilute solutions, a classical Zimm plot provides the z-average radius of gyration (R_g), second virial coefficient (A_2) and weight-averaged relative molar mass ($M_{r,w}$). This is achieved by plotting $H C_m/I(q)$ versus $k' C_m + q^2$. H is a neutron optical constant [$b_v^2 N_a (v_m/M_m)^2$] where b_v^2 is the scattering length density difference between monomer repeat unit and solvent, N_a Avogadro's number, v_m and M_m are the molar volume and molecular mass of a monomer, respectively, all provided in Table I; k' is an arbitrary scaling factor that is independent of the extrapolated quantities^{7,8}.

3.2. Polyelectrolyte Scattering

When a macromolecule contains charged monomers the scattering behavior becomes very different from that of a neutral polymer solution, particularly at low solution ionic strength. This is true for polyelectrolyte gels^{9,10}, charged colloidal particles¹¹, charged dendrimers¹², semi-flexible polyelectrolytes¹³⁻¹⁵, and even linear flexible polyelectrolytes^{11,16}. This paper highlights the behavior as it pertains to photoresist solutions. However, several review articles available^{11,15,16,17,18}.

One feature commonly observed with small-angle neutron scattering by a low-ionic strength semidilute polyelectrolyte solutions is a broad scattering peak at a position of $q_m \neq 0$ indicating a length scale with correlation. This is in contrast to observations in neutral linear homo-polymer mixtures. The scattering behavior from polyelectrolytes to date lacks a successful theory to fit the observable scattering range leading to qualitative structural and thermodynamic parameters. One theory to understand low-ionic strength polyelectrolyte solutions uses a random phase approximation (RPA) that predicts the high- q scattering trend exhibited by polyelectrolytes¹⁸⁻²¹. This theory uses the Debye-Hückel theory to model the interaction potential between two charged statistical segments. The predicted scattering peak position dependence on polymer concentration, salt concentration and temperature qualitatively agree with experiment. However, the RPA prediction fails to agree with experimental data for scaling laws. Its use to extract quantitative information such as the Flory-Huggins interaction parameter has limited success due to several deficiencies (a) anomalous scattering observed in the low- q limit, (b) poor understanding of ionic strength contributions from polymer counter-ions versus added salt ions, (c) effect of density and chain fluctuations, and (d) incomplete consideration of the multi-component nature of the solution. While the molecular mechanism or actual configurational appearance may be in dispute, what is not in dispute is that the origin of the solution structure is electrostatic. Knowing this one can cleverly devise experiments to tune the electrostatic behavior.

One parameter used to quantify electrolyte solutions is the Debye screening length, κ^{-1} . Where κ^2 is the inverse-square Debye length, proportional to the solution ionic strength,

$$\kappa^2 = 4\pi l_B N_a \left(\sum_{\gamma} Z_{\gamma}^2 C_{\gamma} \right) \quad , \quad (2)$$

where the sum over all added electrolyte species γ includes added salts as well as basic ions, and l_B is the Bjerrum length, which is 7 Å at 25 °C in water.

The value of κ^{-1} quantifies the range over which electrostatics are important from any arbitrary test ion. For instance, a 0.26 N solution of TMAH, KOH or NaOH will have κ^{-1} of 6.0 Å, assuming each has the same activity at the equivalent prepared concentrations; this length decreases further to 2.9 Å at 1.1 N. The addition of salt to these basic solutions further decreases the Debye screening length. In principle, once the Debye length is reduced to the length scale of the persistence length, then the system is fully screened.

In the following sections, we will identify a few qualitative polyelectrolyte behaviors present in photoresist materials and discuss them in the context of photoresists in developer solutions.

4. RESULTS AND DISCUSSION

4.1 Photoresist in organic solvent

Due to the low molecular mass of the d₃-PHOST and its contrast with the solvent, neutron scattering provides a reasonable q -range and resolution for such small structures. The scattering by dilute solutions of d₃-PHOST in PGMEA (0.00847, 0.0167, 0.0245, 0.0324, and 0.0645) g cm⁻³ reveals behavior typical of a neutral polymer in an organic solvent, shown in Fig. 1. The scattered intensity decays monotonically with increasing wave vector and the absolute intensity, which is proportional to concentration, increases with increasing concentration.

The results of the Zimm plot for the PHOST in PGMEA shown in Fig. 2 and summarized in Table II, lead to a z -averaged radius of gyration of (30 ± 1) Å, a weight-average relative molar mass of (9600 ± 250) g mol⁻¹ and second virial coefficient of 1.29×10^{-3} cm³mol⁻²g⁻². The second virial coefficient is positive indicating that PGMEA is a good solvent for the d₃-PHOST. We may convert A_2 into the Flory-Huggins interaction parameter χ , where $\chi = 1/2 - A_2\rho_2^2v_1$, ρ_2 is the polymer density and v_1 is the partial molar volume of the solvent²². This interpretation leads to a χ of 0.122 at 25°C. Knowledge of the interaction parameters is needed to understand the effects of swelling at interfaces and the dissolution process because the swelling is a result of the osmotic driving force of solvent into the glassy polymer.

4.2 Photoresist in developer solutions

The d₃-PHOST in the PGMEA casting solvent represents a system with short-ranged interactions in dilute solutions. The experimental observations for the d₃-PHOST in aqueous developer solutions are significantly different. The scattering contrast between the deuterated PHOST and water allows the illustration of the polyelectrolyte effect in Fig. 3. We show 0.0388 g cm⁻³ d₃-PHOST dissolved in 0.26 N TMAH along with the same polymer in PGMEA to demonstrate the difference in phase behavior. The broad peak observed in TMAH is similar to that observed in semidilute polyelectrolyte solutions²³⁻²⁵ and demonstrates that long-ranged electrostatic interactions are present. Even though the mass concentrations are similar, the presence of the peak indicates a strong interaction between polyelectrolyte segments in solution. This strong repulsive interaction leads to a chain expansion beyond its Gaussian theta-coil dimension and has been the subject of numerous investigations²⁶⁻²⁸. These experiments provide the basis of understanding for the role of added salts on the configurational properties of charged polymers, which is directly applicable to photoresist materials in developer solutions.

These observations suggest that in the presence of the aqueous base solution, that is un-buffered, the chemical equilibrium between a protonated and deprotonated state favors the deprotonated hydroxyl form, and can now be considered a polyelectrolyte. This titration of the PHOST monomers results in an ionic character from which the interaction between charged monomers is electrostatic. The remaining basic components, in excess of the titration endpoint, contribute to the solution ionic strength quantified by the Debye screening length (κ^{-1}). This is the starting point to understand resist-developer interactions through the demonstration that the ionization process leads to phase behavior that can not be predicted without considering the electrostatic interactions.

When the electrostatic interactions are screened to short length scales, the phase behavior resembles that of a neutral polymer solution. This was observed in the limit of high salt for flexible polyelectrolytes using SANS²⁹. We demonstrate this behavior in Fig. 4, for the no added salt condition with d₃-PHOST concentration fixed at 0.053 g cm⁻³ in 0.26 N KOH, we observe the scattering peak position, q_m , to be $q_m = (0.0849 \pm 0.0003)$ Å⁻¹. Fixing the d₃-PHOST concentration, an increase in KCl salt concentration to 0.05 M decreases q_m to (0.0781 ± 0.0003) Å⁻¹. For the higher salt concentrations 0.20 M and 0.5 M, a peak is no longer resolved and the scattering form at high salt is similar to that of the neutral polymer solution, which is consistent with a screening of the electrostatic interactions. We provide an estimate for the radius of gyration, R_g , by directly fitting the measured scattered intensity with the Debye structure factor, for the 0.5 M KCl added salt sample, leading to an apparent R_g of (14.0 ± 1.0) Å, which is significantly smaller than the R_g obtained by Zimm plots in PGMEA (30 ± 1) Å or 1.1 N TMAH (29 ± 3) Å (data provided in Table II). This suggests that upon addition of salt the solvent quality is reduced^{30,31} leading to chain contraction, as expected from previous experiments on model charged polymers²⁶⁻²⁸.

This relationship between chain contraction and solvent quality is expected to contribute to the development process and its impact on observed roughness at the developer-resist interface. At sufficiently high ionic strength, the

solvent quality becomes poorer, leading to a decrease in chain dimensions. So, the poor solvent quality will contribute to the observed increased roughness due to increased developer concentration as observed by Reynolds and Taylor³². Thus, the method of choosing the developer could include finding an optimal condition of added salts and base concentration. This source of induced roughness would exacerbate material incompatibility for protected-deprotected components³³. We demonstrate that the polyelectrolyte effects are observed in copolymer solutions as well.

Polyelectrolyte effects are also observed for (5, 10 and 20) % t-BOC protected copolymer in 0.26 N KOH. This is shown in Fig. 5, along with the polymer dissolved in deuterated acetone at the same concentration. In this case we demonstrate that the same experiments can be performed for protonated polymers in deuterated solvents. This experiment indicates that the polyelectrolyte physics is present for copolymers as well as homopolymers. Thus, at the dissolution front the influence of copolymer composition will remain an important variable. We have not explored the transition in miscibility across the anticipated protection limit from which miscibility is expected to undergo a transition, indicative of the “solubility switch.” These experiments are forthcoming, in particular for next generation resists. In the same plot we demonstrate the polyelectrolyte peak is reduced with a constant level of 0.2 M KCl at for each copolymer studied. However, what is not known for these polymers is the extent of association or aggregation due to the copolymer content versus polyelectrolyte effect. The aggregation due to copolymer content needs to be studied in the lower q limit in a more comprehensive manner. The increase in scattered intensity at wave vectors below 0.03 \AA^{-1} is indicative of multi-chain association, typically observed in polyelectrolyte solutions.

We should note that our observations of the equilibrium polyelectrolyte behavior are weakly dependent on the type of aqueous base. For instance we examined PHOSt in three different 0.26 N aqueous base solutions, NaOH, TMAH, and KOH, as shown in Fig. 6. All of these samples show the correlation peak for similar polymer concentrations, denoted in the figure. The peak position is polymer concentration dependent, but a challenge remains to connect the equilibrium structure to observed dissolution rates. The structure is weakly dependent on the type of base used, even though dissolution rate is dependent on base cation and added salts^{35,36}. One connection is through a systematic study of the solvent quality, as it is known that the solvent quality will be a function of added salt or basic species. This solvent quality is then a thermodynamic parameter or driving force for the dissolution³⁴.

Solvent quality should also influence the observed dissolution rate. In particular the observations of the decrease in dissolution rates at sufficient high salt concentrations could also be interpreted as influenced by the reduced solvent quality of the developer solution, since the driving force for the polymer to dissolve is reduced. This is consistent with simple models for neutral polymer dissolution reviewed by Ueberreiter³⁴. However, current models, based upon reaction-rate kinetics, would need to be modified to allow for solvent quality as a parameter in tuning the rate of ionization and rate of polymer migration from the dissolution penetration front. When included, predictions of dissolution rates using equilibrium solution parameters will be possible expanding the ability to predict based upon chemical microstructure in addition to ionization criteria.

5. CONCLUSIONS

This paper demonstrates that PHOSt and copolymers with (5, 15, and 20) % t-BOC protection are polyelectrolytes. Polyelectrolyte effects are induced by the ionization process and quantified by small-angle neutron scattering. The polyelectrolyte effects are absent in organic solvents such as PGMEA and acetone and are observed in aqueous base solutions of 0.26 N TMAH, KOH, and NaOH. The phase behavior and solvent quality are controlled by the solution ionic strength, contributed by the basic ions and added salts. In the case of an excess amount of added salt and/or base the configurational properties of the polymer return to neutral-like behavior and the solvent quality is reduced. In the limit of high ionic strength, we analyze the data using a Zimm plot extracting the second virial coefficient and converting to the Flory-Huggins interaction parameter for PHOSt in PGMEA and 1.1 N TMAH. The radius of gyration of PHOSt in 0.26 N KOH with 0.5 M KCl is reduced to $(14.0 \pm 1.0) \text{ \AA}$ indicating a reduction in size when compared to solutions in base developer solutions without added salts and organic solvents. The influence of solvent quality at the resist-developer interface is in agreement with current experimental data. Increased roughness is observed with increased developer concentration and decreased dissolution rate with high added salt content (related to solvent quality). However these fundamental polyelectrolyte effects will play a more important role, for next generation photoresists that exhibit solvent penetration, swelling, and surface layers. This behavior is minimal for the current 248 nm photoresist investigated as experiments demonstrate surface layer and solvent penetration is lacking or too thin to detect (less than 5 nm).

ACKNOWLEDGMENTS

This work was supported by the Defense Advanced Research Projects Agency under grant N66001-00-C-8083 and the NIST Office of Microelectronics Programs. This work utilized facilities supported in part by the National Science Foundation under Agreement No. DMR-9986442. V.M.P. and R.L.J. acknowledge support by the National Research Council-National Institute of Standards and Technology Postdoctoral Fellowship Program. We acknowledge Raneé Kwong for the GPC measurements on the protonated copolymers.

REFERENCES

1. S. N. Ege, *Organic chemistry, structure and reactivity*, D.C. Heath and Co., Lexington, MA, (1994).
2. H. Ito, IBM Journal of Research and Development **45**, 683 (2001), and SPIE Proceedings, (2003).
3. G.M. Schmid, S.D. Burns, P.C.Tsiartas, and C.G. Willson, J. Vac. Sci. Technol. B **20**, 2913 (2002).
4. F.A. Houle, W.D. Hinsberg, and M.I. Sanchez, *Macromolecules* **35**, 8591 (2002).
5. Certain commercial equipment and materials are identified in this article in order to specify adequately the experimental procedure. In no case does such identification imply recommendation by the National Institute of Standards and Technology, nor does it imply that the material or equipment identified is necessarily the best available for this purpose.
6. <http://rdjazz.nist.gov/programs/sans/manuals/index.html>. G. D. Wignall and F. S. Bates, *Journal of Applied Crystallography* **20**, 28 (1987).
7. J. des Cloizeaux and G. Jannink, *Polymers in solution, their modeling and structure*,(Oxford University Press, New York, 1990).
8. J. S. Higgins, and R. S. Stein, *Journal of Applied Crystallography* **11**, 346 (1978).
9. M. Shibayama, and T. Tanaka, *Journal of Chemical Physics* **102**(23), 9392 (1995).
10. M. Shibayama, F. Ikkai, Y. Shiwa, and Y. Rabin, *Journal of Chemical Physics* **107**(13), 5227 (1997).
11. H. Matsuoka and N. Ise, *Advances in Polymer Science* **114**, 187 (1994).
12. G. Nisato, R. Ivkov, and E. J. Amis, *Macromolecules* **32**, 5895 (1999).
13. M. Milas, M. Rinaudo, R. Duplessix, R.Borsali, and P.Lindner, *Macromolecules* **28**, 3119 (1995).
14. B. Guilleaume, J. Blaul, M. Wittemann, M. Rehahn, and M. Ballauff, **12**, A245-A251 (2000).
15. R. Borsali, H. Nguyen, and R. Pecora, *Macromolecules* **31**, 1548 (1998).
16. H. Dautzenberg, *Polyelectrolytes : formation, characterization, and application*,(Hanser Publishers, New York, 1994).
17. S. Forster, and M. Schmidt, *Advances in Polymer Science* (120), 51 (1995).
18. J.-L. Barrat, and J.-F. Joanny, *Advances in Chemical Physics* (XCIV), 1 (1996).
19. T. A. Vilgis, and R. Borsali, *Physical Review A* **43** (12), 6857 (1991).
20. V. Y. Borue, and I. A. Erukhimovich, *Macromolecules* **21**, 3240 (1988).
21. M. J. Grimson, M. Benmouna, and H. Benoit, *J. Chem. Soc. Faraday Trans. 1* **84**(5), 1563 (1988).
22. *Polymer Handbook*, J.Brandrup and E.H.Immergut (Wiley, New York, 1989).
23. M. Nierlich, C. E. Williams, F. Boue, J. P. Cotton, M. Daoud, B. Farnoux, G. Jannink, C. Picot, M. Moan, C. Wolff, M.Rinaudo, and P. G de Gennes, *Journal De Physique France* **40**, 701 (1979). W. Essafi, F. Lafuma, and

- C. E. Williams, *Structure of Polyelectrolyte Solutions at Intermediate Charge Densities*, ACS Sym. Ser. 548: 278, American Chemical Society, Washington, D.C., 1994.
24. N. Ise, T. Okubo, S. Kunugi, H. Matsuoka, K. Yamamoto, and Y. Ishii, *Journal of Chemical Physics* **81**(7), 3294 (1984).
 25. K. Kaji, H. Urakawa, T. Kanaya, and R. Kitamaru, *J. De Physique France* **49**, 993 (1988).
 26. F. Boue, J. P. Cotton, A. Lapp, and G. Jannink, *J. of Chem. Phys.* **101**(3), 2562 (1994).
 27. M. N. Spiteri, J. P. Cotton, A. Lapp, and G. Jannink, *Phys. Rev. Lett.* **77**(26), 5218 (1996).
 28. V.M. Prabhu, M. Muthukumar, Y.B. Melnichenko and G.D. Wignall, *Polymer* **42**, 8935 (2001).
 29. B. D. Ermi, and E. J. Amis, *Macromolecules* **30**, 6937 (1997).
 30. T. Nicolai, and M. Mandel, *Macromolecules* **22**, 438 (1989).
 31. A. Takahashi., T. Kato, and M. Nagasawa, *J. Phys. Chem.* **71**(7), 2001 (1967).
 32. G.W. Reynolds and J.W. Taylor, *J. Vac. Sci. Technol. B* **17**, 334(1999).
 33. Q. Lin, R. Sooriyakumaran, W.-S. Huang, *Proc. SPIE*, 230, (2000), Q. Lin, D. L. Goldfarb, M. Angelopoulos, S. R. Sriram, J. S. Moore, *Proc. SPIE* (2001),
 34. Ueberreiter, K. *The Solution Process*, Chapter 7, p. 219, in *Diffusion in Polymers*, Ed. J. Crank and G.S. Park, Academic Press, New York, 1968.
 35. P. C. Tsiartas, L. W. Flanagan, W. D. Hinsberg, C. L. Henderson, I. C. Sanchez, R.T. Bonnecaze, and C.G. Willson, *Macromolecules* **30**, 4656 (1997).
 36. H.Y. Shih and A. Reiser, *Macromolecules* **30**, 4353 (1997).

8. FIGURES AND TABLES

Table I. Experimental Quantities

	d ₃ -PHOS _t	h-PHOS _t 5% tBOC	h-PHOS _t 15% tBOC	h-PHOS _t 20% tBOC	PGMEA	d-Acetone	H ₂ O
$M_{r,w}$ [g mol ⁻¹]	8750	10610	10860	10790	-	-	-
$[M_{r,w}/M_{r,n}]$	1.07	1.1	1.09	1.09	-	-	-
M_i [g mol ⁻¹]	123.0	-	-	-	132.16	64.13	18.0
v_i [cm ³ mol ⁻¹]	84.0	-	-	-	136.53	73.54	18.063
b_i [cm]x10 ¹³	60.281	-	-	-	12.42	65.77	-1.675

Table II. SANS Zimm Plot Results

	PGMEA	1.1N TMAH
$M_{r,w}$ [g mol ⁻¹]	9600 ± 250	9648 ± 2000
$\langle R_g^2 \rangle_Z^{1/2}$ [Å]	30 ± 1	29 ± 3
A_2 [cm ³ mol ² g ⁻²]	1.29 × 10 ⁻³	2.7 × 10 ⁻³
χ (25°C)	0.122	0.40

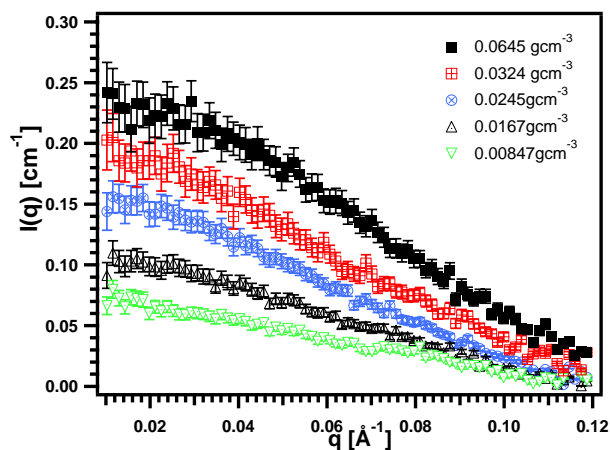


Figure 1. Small-angle neutron scattering by d-PHOS_t in PGMEA. Concentrations are provided in the legend. The scattering behavior is typical of neutral polymer solutions.

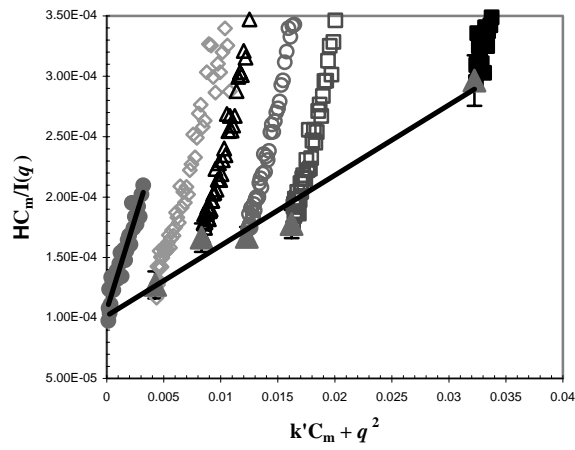


Figure 2. Zimm plot analysis for the scattering by d-PHOSt in PGMEA. The results are a radius of gyration of $30 \pm 1 \text{ \AA}$, weight-average relative molar mass of $9600 \pm 250 \text{ g mol}^{-1}$ and second virial coefficient of $1.29 \times 10^{-3} \text{ cm}^3 \text{ mol}^{-2} \text{ g}^{-2}$. Fits to the data are shown as solid lines which were obtained by a weighted least-squares minimization and the uncertainty is one standard deviation to the fit.

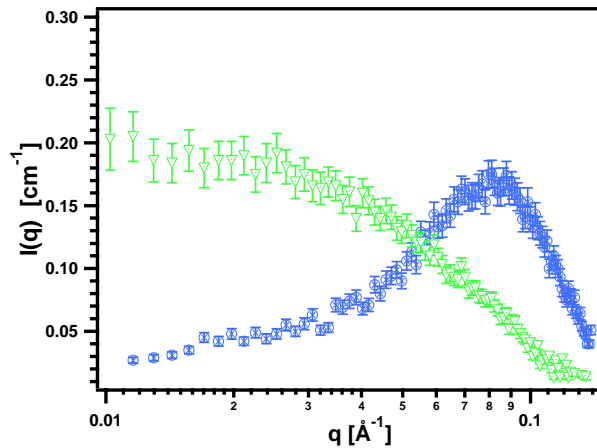


Figure 3. Small-angle neutron scattering by 0.0374 g cm^{-3} d-PHOSt in PGMEA and 0.0388 g cm^{-3} d₃-PHOSt in 0.26 N TMAH, the ▽ and ⊗ symbols, respectively.

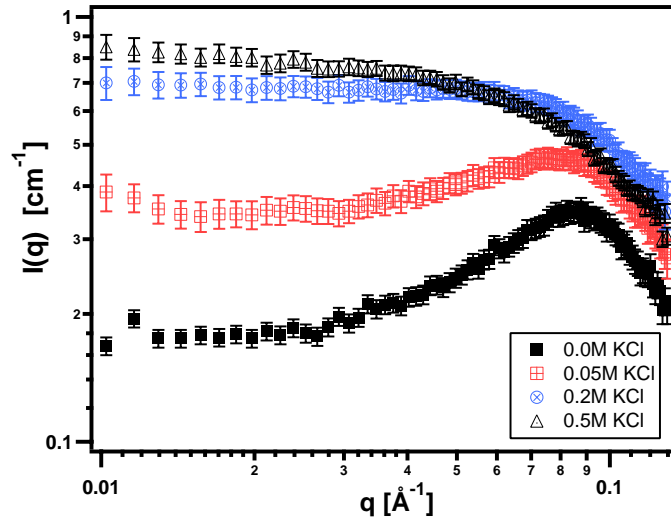


Figure 4. Small-angle neutron scattering by a 0.053 g cm^{-3} d-PHOST in 0.26 M KOH with varying added KCl salt from (0 to 0.5) M, as indicated in the legend, solvent scattering is subtracted. The broadening and elimination of the polyelectrolyte peak is observed, consistent with the screening of the electrostatic interaction.

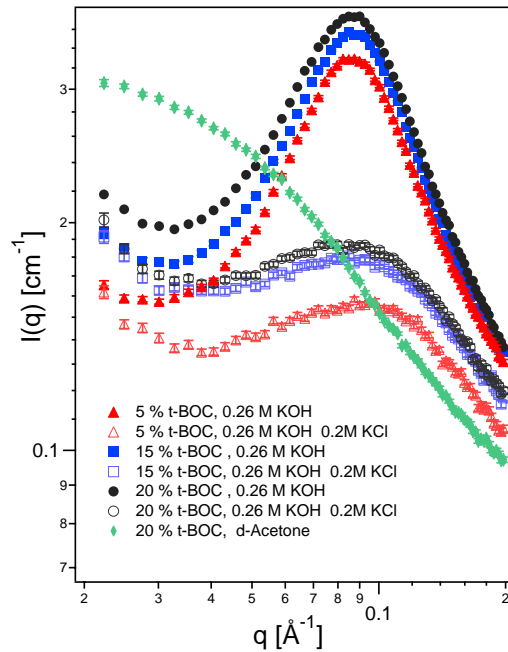


Figure 5. Small-angle neutron scattering by a series of protonated copolymers at a fixed polymer concentration of 0.05 g cm^{-3} . The concentrations of developer and added salts are provided in the legend.

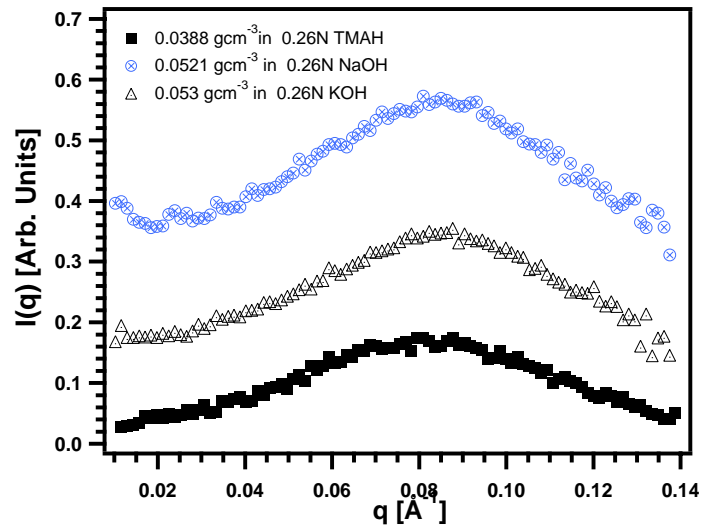


Figure 6. Polyelectrolyte peak for three different aqueous base buffer solutions 0.26 N TMAH, 0.26 N KOH, and 0.26 N NaOH, with (0.0388, 0.0521 and 0.053) g cm^{-3} d_3 -PHOS t concentration, respectively.